TISSUE ENGINEERING: Part A
Volume 24, Numbers 9 and 10, 2018

DOI: 10.1089/ten.tea.2017.0229

termis
Tissue Engineering
& Regenerative Medicine
International Society

ORIGINAL ARTICLE

Phosphate Functional Groups Improve Oligo[(Polyethylene Glycol) Fumarate] Osteoconduction and BMP-2 Osteoinductive Efficacy

Maurits G.L. Olthof, MD,[1–4] Marianna A. Tryfonidou, DVM, PhD,[4] Xifeng Liu, PhD,[2,3] Behdad Pouran, PhD,[1,5] Björn P. Meij, DVM, PhD,[4] Wouter J.A. Dhert, MD, PhD,[1,4] Michael J. Yaszemski, MD, PhD,[2,3] Lichun Lu, PhD,[2,3] Jacqueline Alblas, PhD,[1] and Diederik H.R. Kempen, MD, PhD[6]

Off-the-shelf availability in large quantities, drug delivery functionality, and modifiable chemistry and mechanical properties make synthetic polymers highly suitable candidates for bone grafting. However, most synthetic polymers lack the ability to support cell attachment, proliferation, migration, and differentiation, and ultimately tissue formation. Incorporating anionic peptides into the polymer that mimics acidic proteins, which contribute to biomineralization and cellular attachment, could enhance bone formation. Therefore, this study investigates the effect of a phosphate functional group on osteoconductivity and BMP-2-induced bone formation in an injectable and biodegradable oligo[(polyethylene glycol) fumarate] (OPF) hydrogel. Three types of OPF hydrogels were fabricated using 0%, 20%, or 40% Bis(2-(methacryloyloxy)ethyl) phosphate creating unmodified OPF-noBP and phosphate-modified OPF-BP20 and OPF-BP40, respectively. To account for the osteoinductive effect of various BMP-2 release profiles, two different release profiles (i.e., different ratios of burst and sustained release) were obtained by varying the BMP-2 loading method. To investigate the osteoconductive effect of phosphate modification, unloaded OPF composites were assessed for bone formation in a *bone defect* model after 3, 6, and 9 weeks. To determine the effect of the hydrogel phosphate modification on BMP-2-induced bone formation, BMP-2 loaded OPF composites with differential BMP-2 release were analyzed after 9 weeks of *subcutaneous* implantation in rats. The phosphate-modified OPF hydrogels (OPF-BP20 and OPF-BP40) generated significantly more bone in an orthotopic defect compared to the unmodified hydrogel (OPF-noBP). Furthermore, the phosphate functionalized surface-enhanced BMP-2-induced ectopic bone formation regardless of the BMP-2 release profile. In conclusion, this study clearly shows that phosphate functional groups improve the osteoconductive properties of OPF and enhanced BMP-2-induced bone formation. Therefore, functionalizing hydrogels with phosphate groups by crosslinking monomers into the hydrogel matrix could provide a valuable method for improving polymer characteristics and holds great promise for bone tissue engineering.

Keywords: bone tissue engineering, osteoconduction, bone morphogenetic protein 2, oligo[(polyethylene glycol) fumarate], phosphate functional groups

Introduction

Synthetic polymers are extensively used in tissue engineering.[1] Off-the-shelf availability in large quantities, drug delivery functionality, and modifiable chemistry and mechanical properties make synthetic polymers suitable candidates for bone grafting. However, most polymers were originally developed for nonbiological applications and therefore lack the ability to support cell attachment, proliferation, migration, and differentiation, and ultimately tissue formation.[2]

To mimic the bone extracellular matrix, enable direct biomineralization, and stimulate bone tissue formation, previous research has focused on incorporation of hydroxyapatite

[1]Department of Orthopedics, University Medical Center, Utrecht, The Netherlands.
Departments of [2]Physiology and Biomedical Engineering and [3]Orthopedics, Mayo Clinic College of Medicine, Rochester, Minnesota.
[4]Department of Clinical Sciences of Companion Animals, Faculty of Veterinary Medicine, Utrecht University, Utrecht, The Netherlands.
[5]Department of Biomechanical Engineering, Faculty of Mechanical, Maritime, and Materials Engineering, Delft University of Technology (TU Delft), Delft, The Netherlands.
[6]Department of Orthopaedic Surgery, Onze Lieve Vrouwe Gasthuis, Amsterdam, The Netherlands.

(HA) or other calcium phosphates in synthetic polymers. This major inorganic component of natural bone has been shown to enhance attachment of osteoblasts to synthetic orthopedic implants (osteoconductivity)[3] and may drive osteogenic differentiation of adult human stem cells (osteoinductivity).[4,5]

In general, calcium phosphate mineral coating is time-consuming and results in slow growth of crystalline or amorphous biominerals, which lack adhesion and structural relationship with the polymer substrate.[6–8]

Therefore, more recent studies have focused on developing a more structural bond between the biominerals and polymer substrate, which will ensure a higher level of integration with the newly formed bone.[9,10]

Hydrogels are excellent candidates for designing highly functional tissue engineering scaffolds mimicking the chemical structure of bone. Hydrogel characteristics such as the intrinsic elasticity and high water retention capacities resemble the major extracellular component of bone, that is, collagen.[11] Furthermore, the three-dimensional assembly of hydrogels makes the surface chemistry highly controllable by copolymerization with different monomers displaying multiple functional groups. Since the polymerization chemistry is water compatible, it is possible to incorporate anionic peptides that mimic acidic proteins that can enhance bone mineralization.[12] Therefore, this study investigates the effect of a phosphate functional group on osteoconductivity and Bone Morphogenetic Protein-2 (BMP-2)-induced bone formation in an injectable and biodegradable polyethylene glycol (PEG)-based hydrogel. Oligo(PEG) fumarate (OPF) physical and chemical properties can be modified by incorporation of small cationic or anionic monomers.[13]

Incorporation of bis(2-(methacryloyloxy)ethyl) phosphate (BP) into OPF showed improved mineralization and osteoblast precursor cell attachment, proliferation, and differentiation *in vitro*.[14] Furthermore, BMP-2-induced bone formation may be influenced by differential release profiles in several biomaterials.[15–18] In a previous study, differential BMP-2 release was obtained by modifying the ratio of BMP-2 encapsulated in poly(lactic-co-glycolic acid) (PLGA) microspheres and adsorbed on the hydrogel.[16] To account for the effect of differential BMP-2 on bone formation, two release profiles were investigated for every phosphate modification. Since the *in vitro* cellular function was enhanced in phosphate-containing OPF hydrogels, this study investigates the effect of phosphate functional groups on osteoconduction and BMP-2-induced bone formation *in vivo*.

Materials and Methods

Experimental design

To investigate the effect of phosphate modification on osteoconduction and BMP-2-induced bone formation, OPF hydrogels modified with 0%, 20%, or 40% BP (OPF-noBP, OPF-BP20, and OPF-BP40, respectively) were used. The composites containing PLGA microspheres were used unloaded or BMP-2 loaded. Since BMP-2 release profiles could influence osteoinduction in the various composites, the effect of different release profiles on bone formation was analyzed. To obtain differential *in vivo* BMP-2 release profiles, the protein was either adsorbed on the hydrogel surface and encapsulated in PLGA microspheres (Combined-Cmb, combined burst and sustained release profile) or adsorbed on the hydrogel surface (Adsorbed-Ads, mainly burst release profile) (Table 1).[16]

To investigate the osteoconductive effect of phosphate modification, unloaded OPF composites were assessed for bone formation in a *bone defect* model after 3, 6, and 9 weeks. For the orthotopic site, an additional group was added without implant to show that the femoral defect was critical sized. (Table 1) To determine the effect of the hydrogel phosphate modification on BMP-2-induced bone formation, BMP-2-loaded composites with differential BMP-2 release and corresponding unloaded controls were analyzed after 9 weeks of *subcutaneous* implantation in rats.

Microsphere fabrication

PLGA with a lactic to glycolic ratio of 50:50 (M_w 52 kDa; Evonik, AL) was used to fabricate microspheres using water-in-oil-in-water (W1-O-W2) double-emulsion-solvent-extraction technique according to a previously described method.[19] Briefly, 50 μL of 4 mg/mL BMP-2 solution or 100 μL of ddH_2O was emulsified with 250 mg PLGA 50:50 dissolved in 1.25 mL of dichloromethane using a vortex at 3050 rpm, to create PLGA microspheres loaded with 0.68 μg BMP-2/mg PLGA (Cmb) and unloaded microspheres (Ads). The solution was reemulsified in 2 mL of 2% (w/v) aqueous poly(vinyl alcohol) (PVA, 87–89% mole hydrolyzed, Mw = 13,000–23,000; Sigma Aldrich) to create the double emulsion and added to 100 mL of a 0.3% (w/v) PVA solution and 100 mL of a 2% (w/v) aqueous isopropanol solution. After 1 h of slowly stirring, the PLGA microspheres were collected by centrifugation at 2500 rpm for 3 min, washed thrice with distilled deionized water (ddH_2O), and freeze dried to a free-flowing powder.

Table 1. Characteristics of Study Conditions

	N	*BMP-2 release*	*BP (%w/w OPF), %*	*Implantation site*
Empty	8	—	—	Orthotopic
OPF-noBP	8/8	Unloaded	0	Orthotopic/subcutaneous
OPF-BP20	8/8	Unloaded	20	Orthotopic/subcutaneous
OPF-BP40	8/8	Unloaded	40	Orthotopic/subcutaneous
OPF-noBP-Cmb	8	Burst and sustained	0	Subcutaneous
OPF-noBP-Ads	8	Burst	0	Subcutaneous
OPF-BP20-Cmb	8	Burst and sustained	20	Subcutaneous
OPF-BP20-Ads	8	Burst	20	Subcutaneous
OPF-BP40-Cmb	8	Burst and sustained	40	Subcutaneous
OPF-BP40-Ads	8	Burst	40	Subcutaneous

BP, bis(2-(methacryloyloxy)ethyl) phosphate; OPF, oligo[(polyethylene glycol) fumarate].

Fabrication of composites

OPF was fabricated using PEG with an initial molecular weight of 10 kDa according to previously described method.[14] The OPF composites were fabricated using a salt-leaching method (Fig. 1A).

To create the OPF-noBP paste, OPF (0.5 g/mL), N-vinyl pyrrolidinone (NVP, 0.15 g/mL; Sigma Aldrich, St. Louis, MO), and Irgacure 2959 (I2959, 0.002 g/mL; Ciba-Specialty Chemicals, Tarrytown, NY) were dissolved in ddH_2O. The OPF-BP20 and OPF-BP40 hydrogels reflect 20% w/w OPF and 40% w/w OPF, respectively. To create the OPF-BP20 and OPF-BP40 paste, 200 or 400 mg BP was dissolved in an aqueous solution (OPF [0.5 g/mL], NVP [0.35 g/mL], and I2959 [0.002 g/mL] in ddH_2O). The OPF/NVP or OPF/NVP/BP pastes (22.5% w/w) were mixed with NaCl salt particles (75% w/w, sieved to a maximum size of 300 μm) and PLGA microspheres (2.5% w/w) to create the final paste for the composite. The resulting mixture was forced into a cylindrical mold with dimensions of 3.0 μm diameter and 5.0 μm length and exposed to a UV light (UV-Handleuchte lamp A., Hartenstein, Germany, wavelength: 365 nm, intensity:

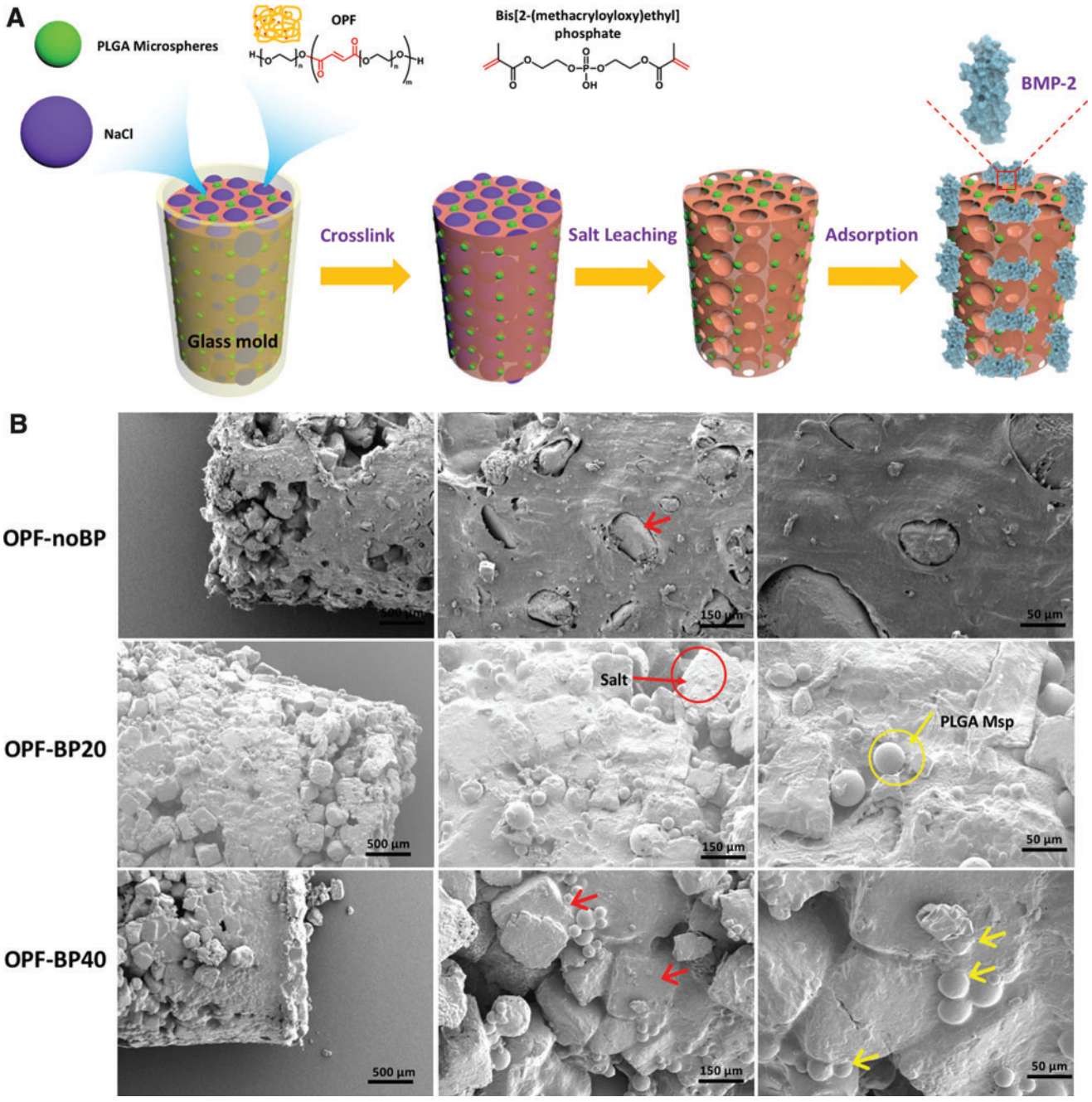

FIG. 1. **(A)** Scheme for the fabrication of the OPF composites. **(B)** SEM images of the OPF composites before salt leaching with salt (*red arrow*) and microspheres (*yellow arrow*) depicted. OPF, oligo[(polyethylene glycol) fumarate]; PLGA, poly(lactic-co-glycolic acid); Msp, microspheres; OPF-noBP, unmodified OPF; OPF-BP20, 20% BP w/w OPF; OPF-BP40, 40% BP w/w OPF; SEM, scanning electron microscopy. Color images available online at www.liebertpub.com/tea

1.2 mW/cm^2, total: 2880 J/cm^2, distance: 3 cm) to crosslink for 40 min. The composites were immersed in sterile ddH_2O to leach out the salt. After blot drying, additional BMP-2 was loaded on the composite matrix by adsorption for the OPF-Cmb and the OPF-Ads scaffolds.

By varying the BMP-2 loading method, two different implants were created consisting of 50% of BMP-2 encapsulated in PLGA microspheres and 50% adsorbed on the composite (OPF-noBP-Cmb, OPF-BP20-Cmb, and OPF-BP40-Cmb: burst release combined with subsequent sustained release), and 100% adsorbed on the composite (OPF-noBP-Ads, OPF-BP20-Ads, and OPF-BP40-Ads: mainly burst release).[16] The loss of BMP-2 by the fabrication method was objectivized in a previous study.[16] This calculation was used to estimate the BMP-2 loss and adjust the applied amount by adsorption. A similar BMP-2 dose and composite fabrication method was used for all OPF composites, which resulted in ~2 μg BMP-2/implant.[16] The release profiles of the two different BMP-2 loading methods is shown in Supplementary Figure S1 (Supplementary Data are available online at www.liebertpub.com/tea). Although this different incorporation process could influence BMP-2 bioactivity, the released BMP-2 remained to show *in vitro* bioactivity comparable to a freshly added BMP-2 dose added to the cell cultures.[16]

Animals and surgical procedure

Thirty-two 16.0 ± 1.2-week-old Harlan Sprague Dawley rats (Envigo, Horst, NL) were used in this study according to an approved protocol by the Dutch Central Committee for animal care and use (protocol: AVD115002015111).

Before surgery, antibiotic prophylaxis (Terramycin/LA, 60 mg/kg; Pfizer, NL) and analgesia (Temgesic, 0.05 mg/kg) were given subcutaneously. Surgery was performed under sterile conditions and general inhalation anesthesia (isoflurane: induction 4%, maintenance ~1.5%). For the orthotopic site, the femur was exposed by a lateral approach and a polyether ether ketone plate (length: 2.3 cm, thickness: 3 mm, width: 3 mm and 6 holes) was fixed to the craniolateral site of the femur using three screws (length: 7 mm, diameter 1 mm) at the proximal end and three screws (length: 7 mm, diameter 1 mm) at the distal end of the plate. The periosteum over ~8 mm of the screw-free mid-diaphysis was removed before removal of a 6-mm long bone segment using a tailor-made saw guide and a wire saw (RatFix, AO Foundation).

Following closure of the femoral wound, subcutaneous pockets were created in the thoracolumbar region and filled with BMP-2-loaded implants and corresponding unloaded controls. Temgesic (0.05 mg/kg) was given subcutaneously as postoperative analgesia for 3 days, twice daily. After 9 weeks, the rats were euthanized by CO_2 asphyxiation to collect the implants for assessment of bone formation by micro-computed tomography (μ-CT) and subsequent histological analysis.

Quantification of bone volume

Micro computed tomography (μCT) was used to determine the total bone volume within the scaffolds in the orthotopic and ectopic location. *In vivo* scanning under general anesthesia (isoflurane: induction 4%, maintenance ~1.5%) was performed at 3, 6, and 9 weeks using a

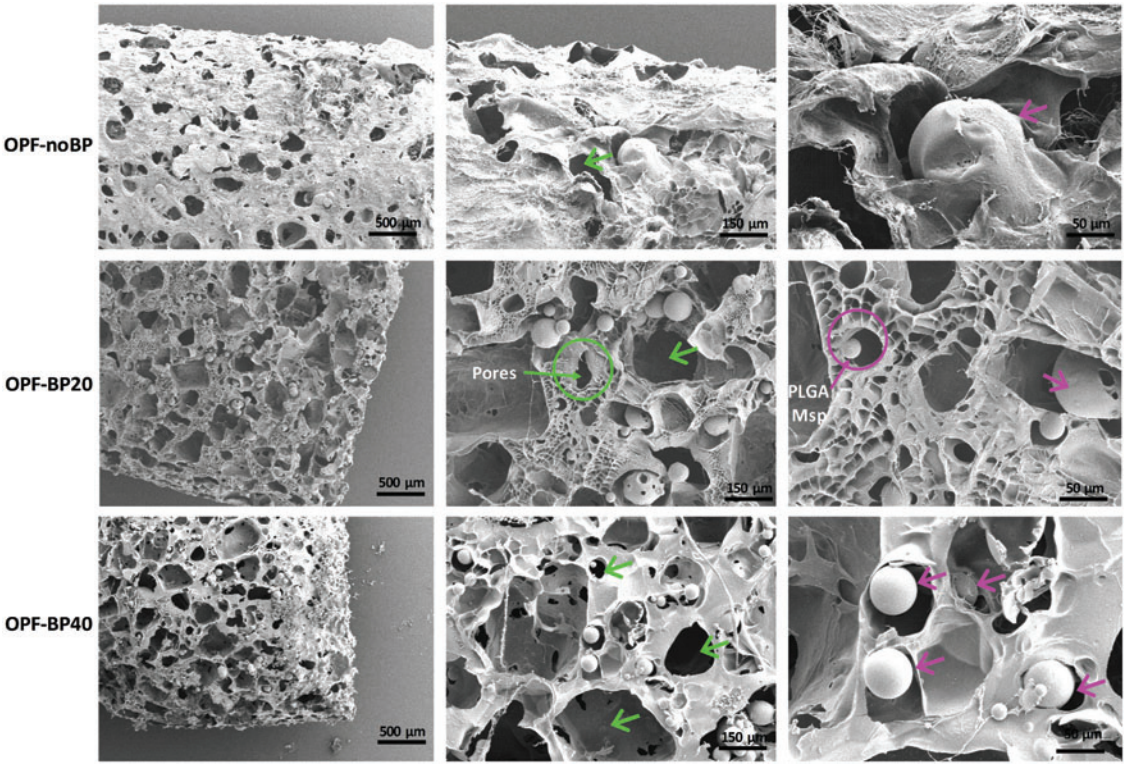

FIG. 2. SEM images of the OPF composites with pores (*green arrow*) and PLGA microspheres (*purple arrow*) depicted. PLGA, poly(lactic-co-glycolic acid); Msp, microspheres; OPF-noBP, unmodified OPF; OPF-BP20, 20% BP w/w OPF; OPF-BP40, 40% BP w/w OPF; SEM, scanning electron microscopy. Color images available online at www.liebertpub.com/tea

Quantum FX (Perker Elmer) scanner at 42 μm^3 voxel size, 3 min scan time, 90 kV tube voltage, and 180 μA tube current. *Ex vivo* scanning after 9 weeks was performed to analyze the subcutaneous implants. Global thresholding was applied in *ImageJ* (version 2.0.0) to quantify the bone formation (*BoneJ*, plugin of *ImageJ*) within the implants. The results are given in bone volume (mm^3) and % of bone volume normalized to the total known defect volume.

Histology

After μ-CT, tissues were fixed in formalin and dehydrated in graded series of ethanol, and embedded in methylmethacrylate. Qualitative assessment was performed in 30 μm thick methylene blue-/basic fuchsin-stained sections for evaluation of general tissue response and bone formation.

Statistical analysis

Statistical analysis was performed in SPSS 22.0 (SPPS, Inc., Chicago, IL). *In vivo* results ($n=8$) are given as means ± standard deviations (SD). Before the *in vivo* study, power analysis estimated that, to demonstrate a relevant difference of at least 20% at an alpha of 0.05 and an SD of 1.4, the groups should be $n=8$ per condition at a power of 80%. The change in bone volume over time is calculated in bone volume increase/week for every 3 weeks. All datasets were tested for outliers using Hoaglin's outlier labeling

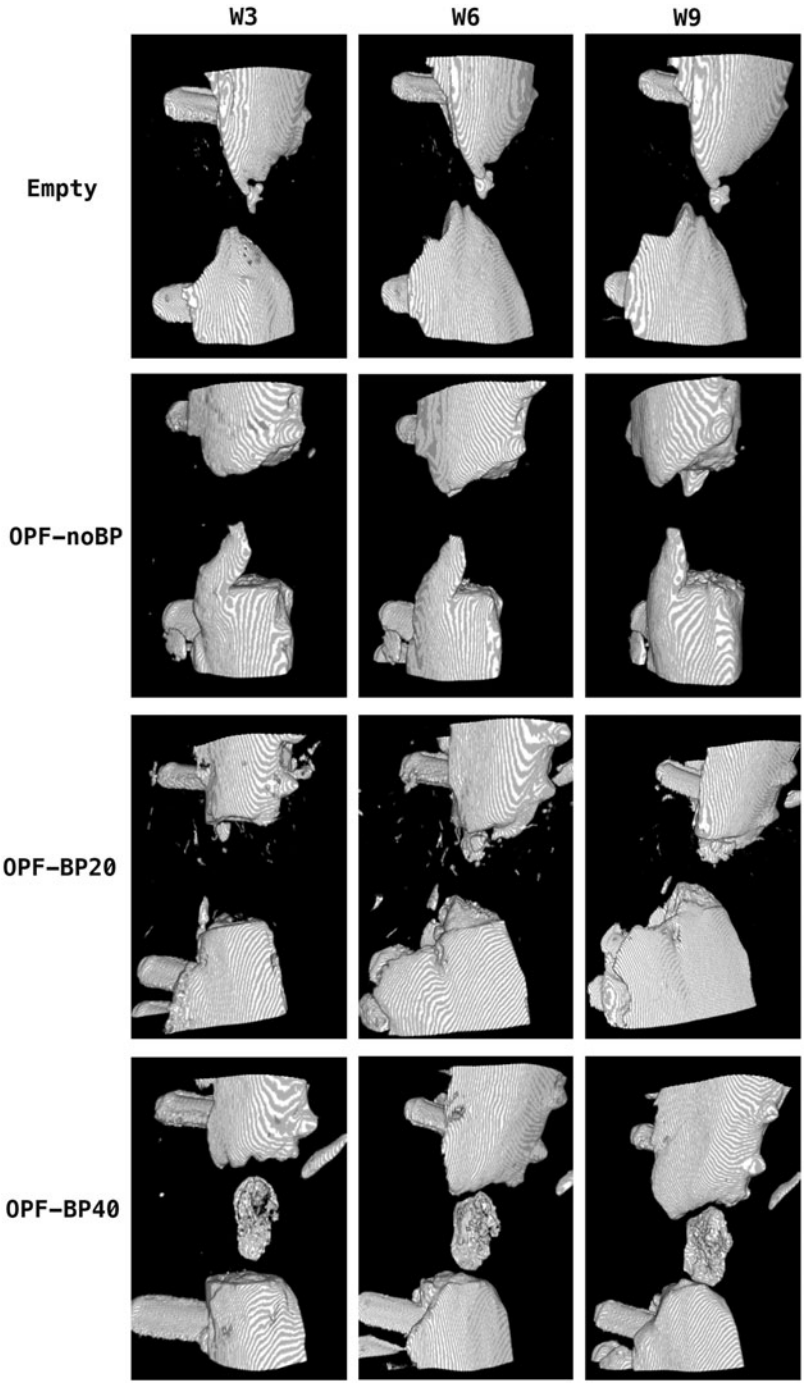

FIG. 3. Three-dimensional μ-CT reconstructions of the bone defects after 3, 6, and 9 weeks. Empty, unfilled defect; OPF-noBP, unmodified OPF; OPF-BP20, 20% BP w/w OPF; OPF-BP40, 40% BP w/w OPF; μ-CT, micro-computed tomography.

rule,[20] for normality of the residuals using the Shapiro-Wilk test and for homogeneity of variances using the Levene's test. Parametric data were analyzed using univariate analysis of variances followed by Benjamini Hochberg *post-hoc*. Differences were considered significant for $p < 0.05$.

Results

Composites characterization

Scanning electron microscopy (SEM) images of the OPF hydrogels before salt leaching (Fig. 1B) showed microspheres and salt particles embedded in the polymer matrix. Salt leaching resulted in a highly porous interconnected network with microspheres randomly distributed in the polymer matrix for all hydrogel modifications (Fig. 2).

Animals

One rat died during surgery and another during *in vivo* μ-CT measurements due to overdose of used anesthetics. Furthermore, in a third rat, bone defect could not be created due to overdrilling of screw holes. These three rats had to be excluded from further analysis.

Analysis of bone formation

Osteoconductivity. For the *orthotopic* application site, μ-CT showed nonbridging defects with bone ingrowth proximally and distally to the critical sized defects (Fig. 3). Significantly ($p < 0.04$) more bone volume was observed in the empty defect ($13.5 \pm 5.6\,mm^3$ or $18\% \pm 0.1\%$) compared to OPF-noBP ($6.7 \pm 3.6\,mm^3$ or $9\% \pm 0.1\%$) after 3 weeks (Fig. 4A). No differences were observed between OPF-BP20 ($8.0 \pm 2.7\,mm^3$ or $11\% \pm 0.1\%$) and OPF-BP40 ($9.7 \pm 6.7\,mm^3$ or $13\% \pm 0.1\%$) for this time period. After 6 weeks, both the empty defect ($19.9 \pm 8.1\,mm^3$ or $26\% \pm 0.1\%$) and OPF-BP20 ($17.9 \pm 6.6\,mm^3$ or $24\% \pm 0.1\%$) contained more ($p < 0.02$) bone compared to OPF-noBP ($9.1 \pm 5.6\,mm^3$ or $12\% \pm 0.1\%$). Subsequently, after 9 weeks, a higher ($p < 0.03$) bone volume was observed in the empty defect, ($24.0 \pm 9.1\,mm^3$ or $32\% \pm 12\%$) OPF-BP20 ($25.9 \pm 9.8\,mm^3$ or $35\% \pm 13\%$) and OPF-BP40 ($25.5 \pm 9.8\,mm^3$ or $34\% \pm 13\%$) compared to OPF-noBP ($12.7 \pm 7.6\,mm^3$ or $17\% \pm 10\%$). No significant differences were seen between the empty defect, OPF-BP20 and OPF-BP40.

To visualize differences in bone formation in time between groups, the difference in bone volume within each group between time points was calculated (Fig. 4B). A higher ($p = 0.04$) bone formation rate was seen in the empty defect compared to OPF-noBP after 3 weeks. After 6 weeks, OPF-BP20 showed a higher ($p = 0.01$) bone formation rate compared to OPF-noBP. For the 9-week time point, a higher ($p = 0.02$) bone formation rate was seen in OPF-BP40 compared to both empty defect and OPF-noBP.

Osteoinductivity. *Subcutaneously*, no bone volume was seen in the scaffolds without BMP-2 (data not shown in graph). No significant differences in bone volume were observed between the different BMP-2 loading methods.

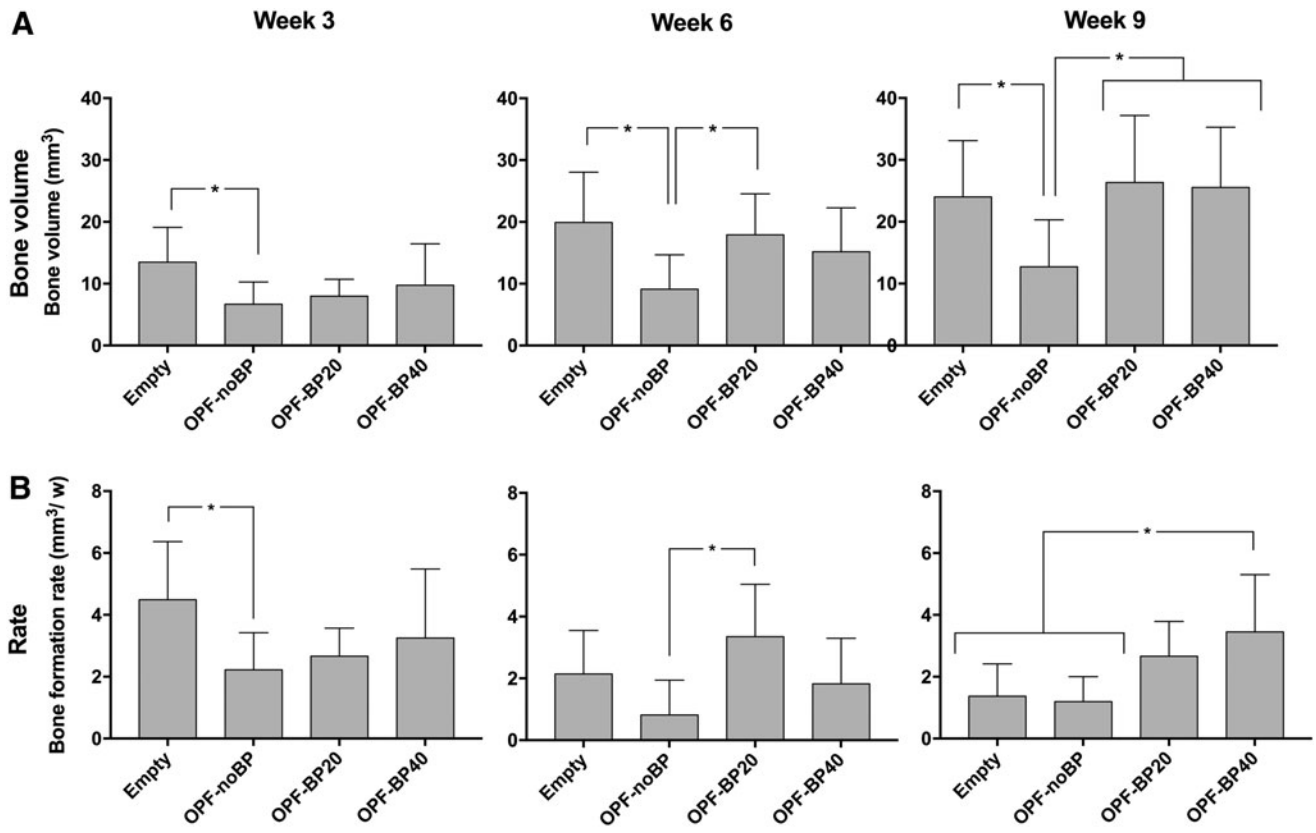

FIG. 4. Amount of newly formed bone in the orthotopic defect after 3, 6, and 9 weeks of implantation, **(A)** shown in volume mean ± Standard deviation (mm^3). The bone formation rate every 3 weeks (mm^3/week) **(B)**. *Significant difference at $p < 0.05$. Empty, unfilled defect; OPF-noBP, unmodified OPF; OPF-BP20, 20% BP w/w OPF; OPF-BP40, 40% BP w/w OPF.

While the phosphate-modified composites generated more ($p < 0.001$) bone compared to unmodified composites, no differences were seen between OPF-BP20 and OPF-BP40 composites (Fig. 5).

Histology

Osteoconductivity. After 9 weeks of *orthotopic* implantation, no signs of persistent inflammatory response were observed across all groups (Fig. 6). In the empty defect, an interposition of muscle tissue was observed at the center of the defect with bone ingrowth distal and proximal in the defect. Unmodified OPF-noBP showed little cellular infiltration with large total area of void volume (>50% pore volume) and minimal woven bone ingrowth at the edges of the defect. In both phosphate-modified OPF-BP20 and OPF-BP40 composites, proper cellular and blood vessel infiltration (>75% pore volume) were observed with woven combined with lamellar bone regeneration in direct contact with the hydrogel surface.

Osteoinductivity. After 9 weeks of *subcutaneous* implantation, unloaded OPF-noBP and OPF-noBP-Ads showed similar tissue formation as the orthotopic location, with minimal cellular infiltration and a large area of void volume (>50% pore volume) (Fig. 7). Only in OPF-noBP-Cmb, minimal woven bone was observed. Unloaded OPF-BP20 and OPF-BP40 showed substantial cellular infiltration (>75% pore volume) without bone formation. Regardless of the BMP-2 release profile, the BMP-2-loaded OPF-BP20 and OPF-BP40 composites showed substantial bone formation, with woven bone in direct contact with the hydrogel surface.

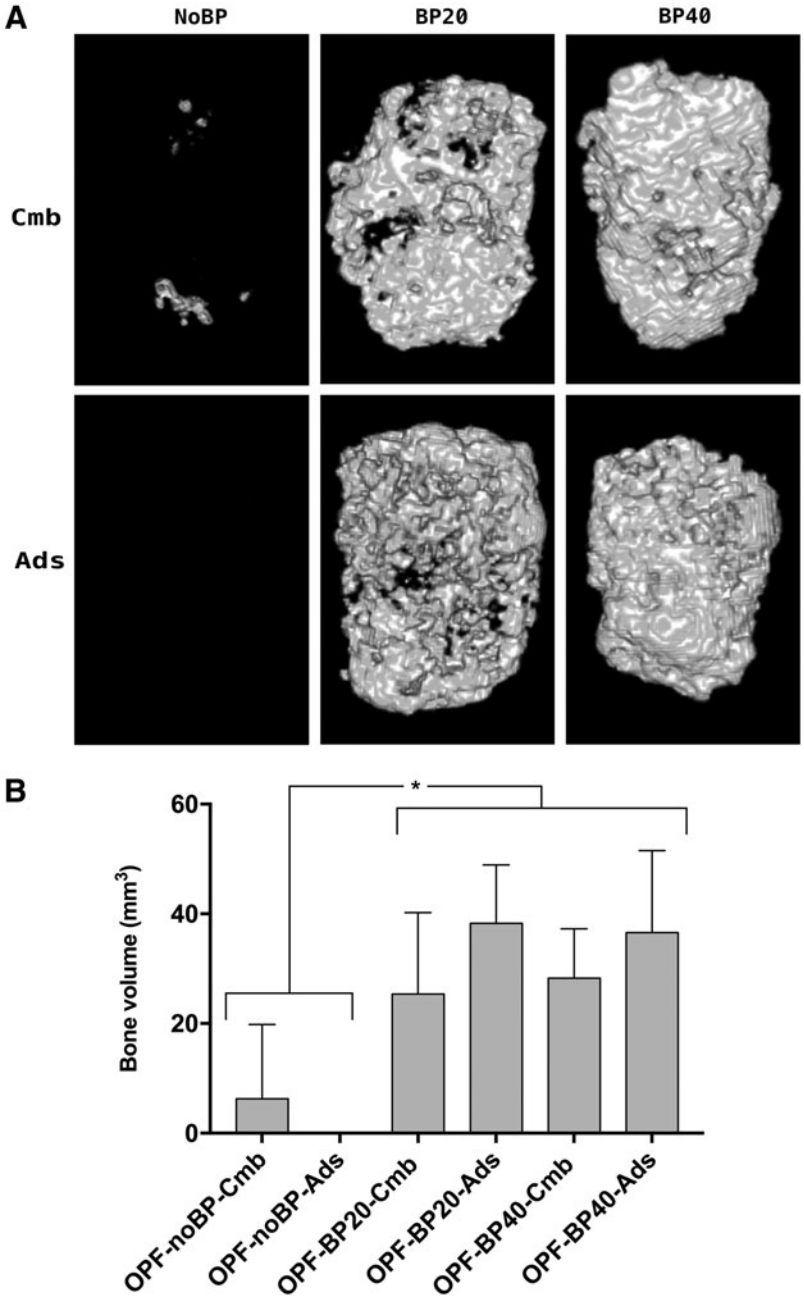

FIG. 5. Three-dimensional μ-CT reconstructions of the implants after 9 weeks **(A)**. Amount of newly formed bone after 9 weeks of subcutaneous implantation **(B)**, shown in mean volume ± SD (mm^3). *Significant difference at $p < 0.05$. OPF-noBP, unmodified OPF; OPF-BP20, 20% (w/w) BP in OPF; OPF-BP40, 40% (w/w) BP in OPF. Cmb, combined BMP-2 release; Ads, mainly BMP-2 burst release; μ-CT, micro-computed tomography. All implants contain 2 μg BMP-2.

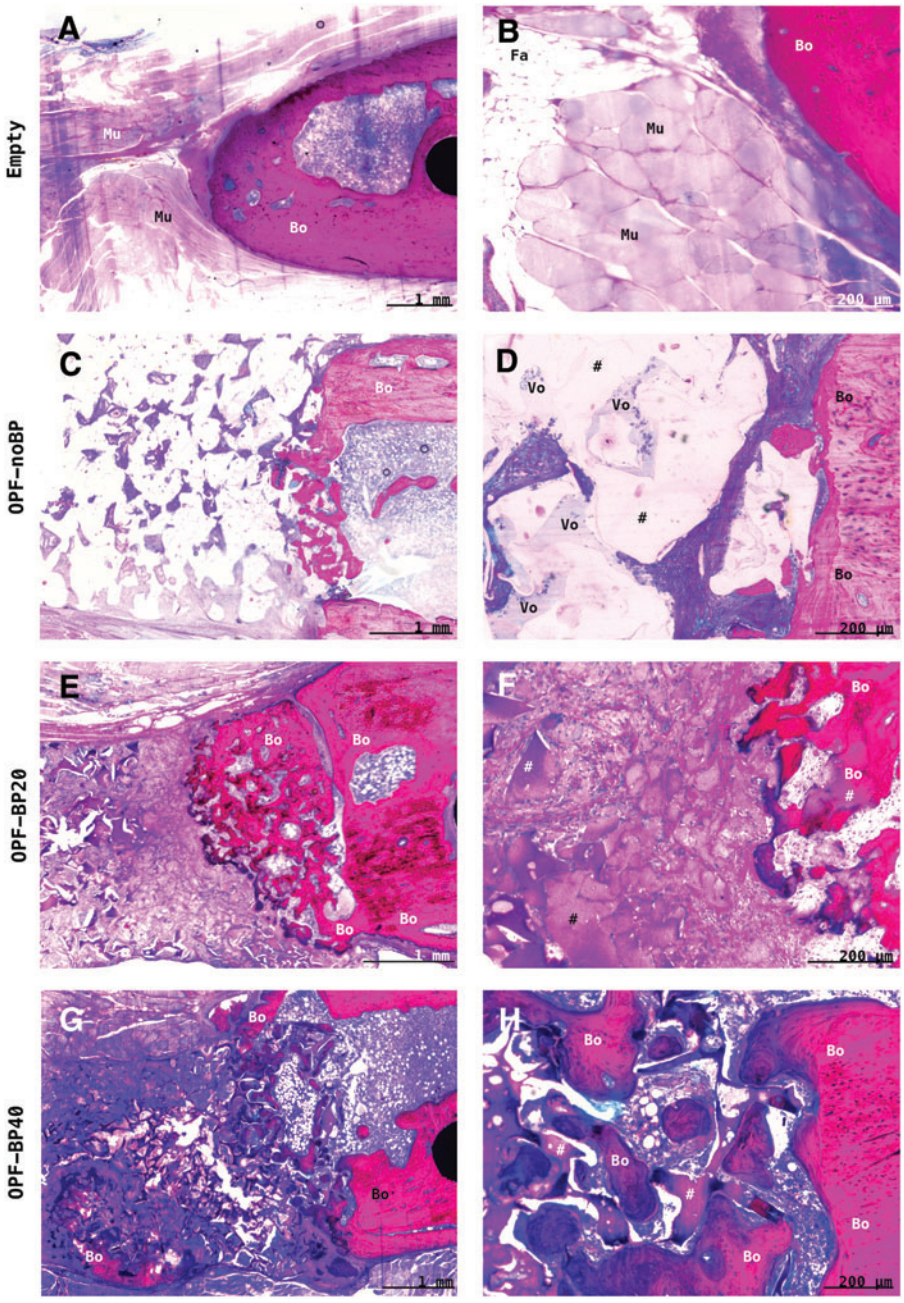

FIG. 6. Representative methylene blue-/basic fuchsin-stained histological sections of the implants after 9 weeks of *orthotopic* implantation. In the empty defect **(A, B),** there was interposition of muscle (Mu) and fat (Fa) tissue in the center of the empty femoral defect with limited ingrowth of bone (Bo) from the distal and proximal osteotomy sides. The unmodified OPF-noBP (#) **(C, D)** showed minimal cellular infiltration and much void volume (Vo) with minimal bone ingrowth at the edges of the defect. In both phosphate-modified OPF-BP20 **(E, F)** and OPF-BP40 **(G, H),** good cellular and blood vessel infiltration (>75% pore volume) were observed with bone regeneration in direct contact with the hydrogel surface (#). Empty, unfilled defect; OPF-noBP, unmodified OPF; OPF-BP20, 20% BP w/w OPF; OPF-BP40, 40% BP w/w OPF. Color images available online at www.liebertpub.com/tea

Discussion

This study clearly shows that the phosphate functionalized surface-enhanced BMP-2 induced ectopic bone formation. Even more so, phosphate functional groups enhance the osteoconductive characteristics of OPF in an orthotopic defect.

Incorporation of phosphate functional groups increased the osteoconductive properties of OPF. Since bonelike minerals have shown to be a prerequisite for osteoconduction,[3] biomineralization is thought to be the important underlying mechanism. Natural biomineralization of collagen fibrils can be mimicked by incorporation of functional anionic groups within the polymer network.[21] Anionic groups with strong affinity to calcium can both adsorb HA and trigger the physiologic process of nucleation. This provides a strong interaction between the organic matrix of the polymer substrate with the inorganic phase of natural bone. Several anionic functionalized groups, including carboxyl, phosphate, phosphonate, hydroxyl, and sulfate groups, showed strong adhesion to HA and improved biomineralization and cellular adhesion to the synthetic polymer *in vitro*.[12] Various polymers functionalized with phosphate groups showed improved peptide specificity for bone-like minerals and improved biomineralization.[22–24]

Although the *in vitro* results of phosphate-modified synthetic hydrogels have been promising, no *in vivo* studies were available studying the effect of functionalized phosphate groups on bone formation. The improved *in vivo* osteoconductive properties of phosphate-modified OPF in this study show that phosphate-functionalized polymers hold great promise for bone regeneration.

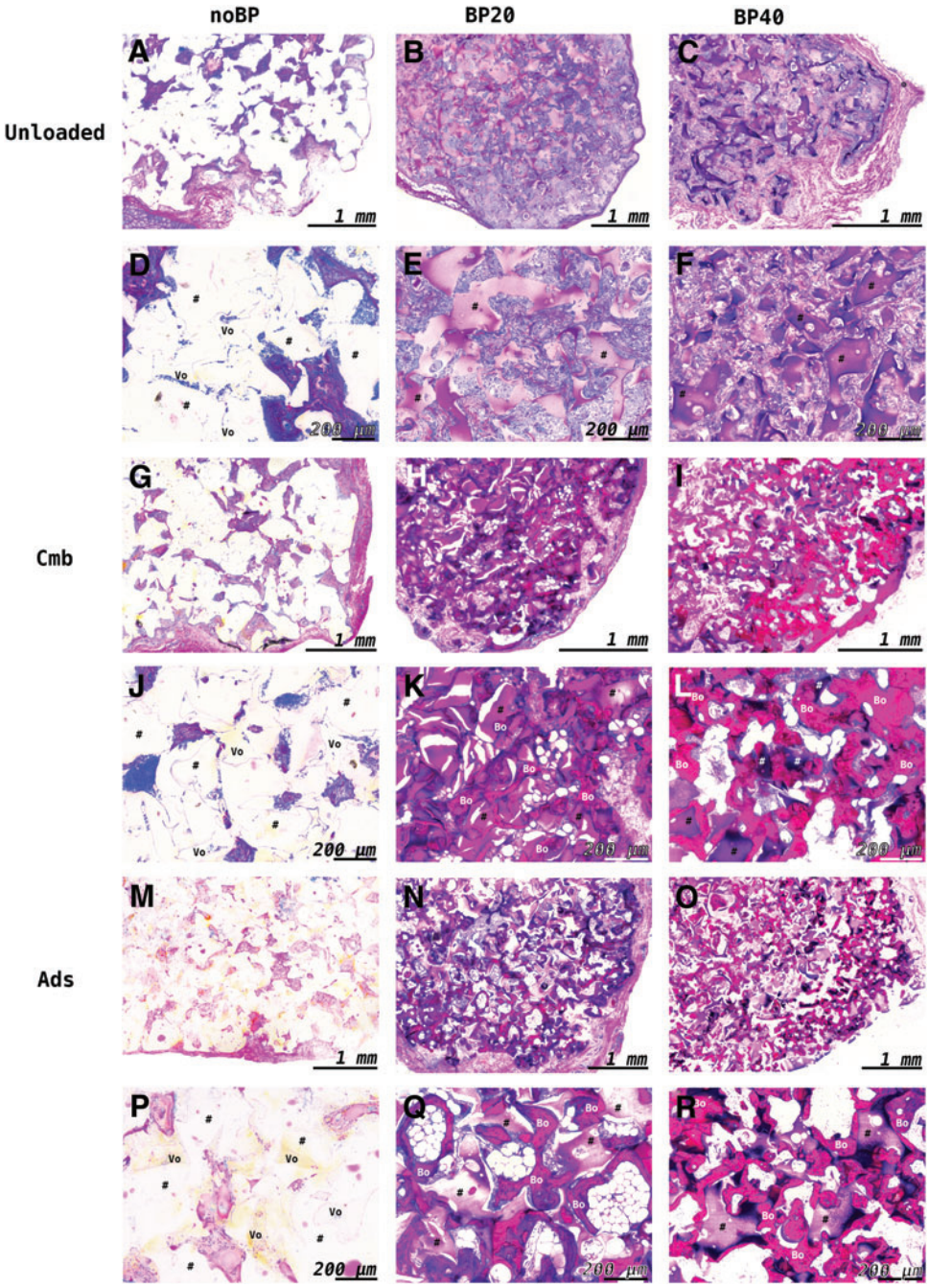

FIG. 7. Representative methylene blue-/basic fuchsin-stained histological sections of the implants (#) after 9 weeks of *subcutaneous* implantation. Unloaded OPF-noBP composites **(A, D)** showed minimal cellular infiltration with much void (Vo) volume (>50%). While OPF-noBP-Ads **(M, P)** showed no bone formation, minimal bone was observed in OPF-noBP-Cmb **(G, J)**. Unloaded BP-modified composites **(B, C, E, F)** showed substantial cellular infiltration without bone tissue. BMP-2-loaded BP-modified composites **(H, I, K, L, N, O, Q, R)** showed substantial bone formation (Bo) with woven bone in direct contact with the polymer surface. noBP, unmodified OPF; BP20, 20% BP w/w OPF; BP40, 40% BP w/w OPF. Unloaded, not loaded with BMP-2; Cmb, combined BMP-2 release; Ads, mainly BMP-2 burst release. Color images available online at www.liebertpub.com/tea

Similar bone formation was seen for the empty defect compared with the phosphate-modified hydrogels in the absence of BMP-2. While the bone formation in the empty defect started at a high rate and decreased rapidly over time, the bone growth in the phosphate-functionalized hydrogels started at a low rate, but was stable over time. The osteoconductive properties of the phosphate-modified hydrogels allow slow ingrowth of bone into the polymer porous structure without interposition of the tissue environment into the defect, while interposition of muscle and fat tissue could have prohibited the empty defect from bridging. The unmodified OPF-noBP showed that nonosteoconductive materials in bone defects allow minimal bone ingrowth and have a negative influence on bone regeneration.

Phosphate functional groups enhanced BMP-2-induced ectopic bone formation. Previous studies showed that the surface of PEG-based hydrogels is not well suited for cellular attachment and biomineralization.[14,25] Also, in this study, the unmodified hydrogel showed a limited amount of ectopically formed bone and inferior osteoconductive properties compared to empty defects and phosphate-modified OPF.

In vitro, a phosphate functionalization of OPF showed significant improvement in cell attachment, proliferation, and differentiation of osteoblast precursor cells. *In vivo*, no ectopic bone formation was seen in the negative controls without BMP-2, indicating phosphate-modified polymers are not osteoinductive in an ectopic location. While minimal bone formation was seen in BMP-2-loaded unmodified

polymers, substantial bone formation was observed in BMP-2-loaded OPF-BP20 and OPF-BP40 composites. Within the phosphate modifications, a trend could be observed with a more sustained BMP-2 release increasing bone formation in noBP composites and a mainly burst release increasing bone formation in BP-modified composites. However, the limited effect on bone formation indicates that the effect of BMP-2 release profiles is supplementary to the effect of phosphate modifications in these composites. Previous research also showed that calcium phosphate coatings in combination with BMP-2 improve bone formation in a synthetic polymer.[26]

Since the BMP-2 release profiles were similar for the different composites. In this study, the observed difference in BMP-2-induced bone formation could be explained by cell-composite or BMP-2-composite interaction. It is tempting to hypothesize that an enhanced ectopic bone formation is attributed to improved cell adhesion and proliferation. Furthermore, the biomimetic surface of the phosphate-modified hydrogels may have improved the adsorption of certain cytokines and growth factors, which could have had a synergistic effect with BMP-2 on bone formation.[27] As such, the improved BMP-2 osteoinductivity of phosphate-modified hydrogels can help lower growth factor dose in future clinical applications.

Crosslinking a phosphate-containing monomer into the OPF hydrogel matrix provides an efficient and effective method for functionalizing the hydrogel surface for bone grafting. Coating techniques are widely used to improve the biomimetic properties of synthetic polymers. Weak adhesion, lack of structural integrity, and long processing time make these techniques a method with minimum quality and efficiency.[6–8]

Furthermore, these coated scaffolds are less suitable for off-the-shelf products that can be shaped into the desired size of a clinical bone defect. Therefore, studies focus on encapsulating calcium phosphate microparticles into the polymer matrix to mimic the bone inorganic phase.[28–30] However, this method will not result in mimicking the hierarchically structured HA nanocrystallites, seen in organic matrix of bone. Therefore, newer methods focus on chemically altering the polymer interface.

While some methods involve chemical post processing treatment, other methods incorporate monomers with functional groups in the polymer matrix.[12] While both methods improve the integration of calcium phosphate with the polymer surface and enhance biomineralization, preferably no time-consuming postprocessing is needed. Functionalizing polymers by incorporation of phosphate functional groups was shown to be effective in several polymers.[22,23] This implies that incorporation of phosphate-functionalized groups into a polymer could be an efficient and effective method for functionalizing polymers for bone grafting.

Incorporation of more phosphate functional groups than 20% w/w did not stimulate further osteoconduction and BMP-2-induced bone formation. *In vitro*, higher amounts of phosphate on the surface decreased the Ca/P ratio of the adsorbed minerals.[14] This could indicate that Ca^{2+} binds less efficiently to a higher phosphate surface density and will not contribute to a higher biomineralized surface. Furthermore, increasing the phosphate content of OPF above 20% wt. did not have an additional effect on the *in vitro* proliferation of osteoblasts.[14] These results may indicate that above a certain threshold density, a phosphate functionalized surface is not contributing to an improved bone formation.

In conclusion, this study clearly shows that phosphate functional groups improve the osteoconductive properties of OPF. Furthermore, the phosphate-functionalized surface enhanced bone formation in the context of BMP-2. Therefore, functionalizing hydrogels with phosphate groups by crosslinking monomers into the hydrogel matrix could provide a valuable method for improving polymer characteristics and holds great promise for bone tissue engineering.

Acknowledgments

The authors acknowledge the financial support from the National Institutes of Health (R01 AR45871 and R01 EB03060), the AO Foundation (AO startup grant S-15-46K), the Dutch Arthritis Foundation (LLP12 and LLP22), and Anna-NOREF foundation. Furthermore, the authors thank Nynke Ankringa from the Department of Veterinary Pathology of the University of Utrecht for analyzing histology, and Loek Loozen, Michiel Croes, and Marianne K. E. Koolen from the Department of Orthopedic Surgery of the University Medical Center Utrecht for assisting with the surgery.

Disclosure Statement

The authors declare no conflicts of interest.

References

1. Kohane, D.S., and Langer, R. Polymeric biomaterials in tissue engineering. Pediatr Res **63,** 487, 2008.
2. Rezwan, K., Chen, Q.Z., Blaker, J.J., and Boccaccini, A.R. Biodegradable and bioactive porous polymer/inorganic composite scaffolds for bone tissue engineering. Biomaterials **27,** 3413, 2006.
3. Hench, L.L. Bioceramics: from concept to clinic. J Am Ceram Soc **74,** 1487, 1991.
4. Ohgushi, H., and Caplan, A.I. Stem cell technology and bioceramics: from cell to gene engineering. J Biomed Mater Res **48,** 913, 1999.
5. Krebsbach, P.H., Kuznetsov, S.A., Satomura, K., Emmons, R.V., Rowe, D.W., and Robey, P.G. Bone formation in vivo: comparison of osteogenesis by transplanted mouse and human marrow stromal fibroblasts. Transplantation **63,** 1059, 1997.
6. Kokubo, T. Apatite formation on surfaces of ceramics, metals and polymers in body environment. Acta Mater **46,** 2519, 1998.
7. Rhee, S.-H., and Tanaka, J. Effect of citric acid on the nucleation of hydroxyapatite in a simulated body fluid. Biomaterials **20,** 2155, 1999.
8. Saiz, E., Goldman, M., Gomez-Vega, J.M., Tomsia, A.P., Marshall, G.W., and Marshall, S.J. In vitro behavior of silicate glass coatings on Ti6Al4V. Biomaterials **23,** 3749, 2002.
9. Song, J., Saiz, E., and Bertozzi, C.R. A new approach to mineralization of biocompatible hydrogel scaffolds: an efficient process toward 3-dimensional bonelike composites. J Am Chem Soc **125,** 1236, 2003.
10. Murphy, W.L., and Mooney, D.J. Bioinspired growth of crystalline carbonate apatite on biodegradable polymer substrata. J Am Chem Soc **124,** 1910, 2002.
11. Peppas, N.A. Hydrogels in Medicine and Pharmacy. Boca Raton, FL: CRC Press, 1988.

12. Farbod, K., Nejadnik, M.R., Jansen, J.A., and Leeuwenburgh, S.C. Interactions between inorganic and organic phases in bone tissue as a source of inspiration for design of novel nanocomposites. Tissue Eng Part B Rev **20,** 173, 2014.
13. Dadsetan, M., Pumberger, M., Casper, M.E., *et al.* The effects of fixed electrical charge on chondrocyte behavior. Acta Biomater **7,** 2080, 2011.
14. Dadsetan, M., Giuliani, M., Wanivenhaus, F., Brett Runge, M., Charlesworth, J.E., and Yaszemski, M.J. Incorporation of phosphate group modulates bone cell attachment and differentiation on oligo(polyethylene glycol) fumarate hydrogel. Acta Biomater **8,** 1430, 2012.
15. van de Watering, F.C., Molkenboer-Kuenen, J.D., Boerman, O.C., van den Beucken, J.J., and Jansen, J.A. Differential loading methods for BMP-2 within injectable calcium phosphate cement. J Control Release **164,** 283, 2012.
16. Olthof, M.G., Kempen, D.H., Liu, X., *et al.* Bone morphogenetic protein-2 release profile modulates bone formation in phosphorylated hydrogel. J Tissue Eng Regen Med 2018 [Epub ahead of print]; DOI: 10.1002/term.2664.
17. Yamamoto, M., Takahashi, Y., and Tabata, Y. Controlled release by biodegradable hydrogels enhances the ectopic bone formation of bone morphogenetic protein. Biomaterials **24,** 4375, 2003.
18. Kempen, D.H., Lu, L., Hefferan, T.E., *et al.* Retention of in vitro and in vivo BMP-2 bioactivities in sustained delivery vehicles for bone tissue engineering. Biomaterials **29,** 3245, 2008.
19. Kempen, D.H., Lu, L., Classic, K.L., *et al.* Non-invasive screening method for simultaneous evaluation of in vivo growth factor release profiles from multiple ectopic bone tissue engineering implants. J Control Release **130,** 15, 2008.
20. Hoaglin, D.C., Iglewicz, B., and Tukey, J.W. Performance of some resistant rules for outlier labeling. J Am Stat Assoc **81,** 991, 1986.
21. Wang, Y., Azaïs, T., Robin, M., *et al.* The predominant role of collagen in the nucleation, growth, structure and orientation of bone apatite. Nat Mater **11,** 724, 2012.
22. Suzuki, S., Whittaker, M.R., Grøndahl, L., Monteiro, M.J., and Wentrup-Byrne, E. Synthesis of soluble phosphate polymers by RAFT and their in vitro mineralization. Biomacromolecules **7,** 3178, 2006.
23. Kim, C.W., Kim, S.E., Kim, Y.W., *et al.* Fabrication of hybrid composites based on biomineralization of phosphorylated poly(ethylene glycol) hydrogels. J Mater Res **24,** 50, 2009.
24. Addison, W.N., Miller, S.J., Ramaswamy, J., Mansouri, A., Kohn, D.H., and McKee, M.D. Phosphorylation-dependent mineral-type specificity for apatite-binding peptide sequences. Biomaterials **31,** 9422, 2010.
25. Nuttelman, C.R., Benoit, D.S., Tripodi, M.C., and Anseth, K.S. The effect of ethylene glycol methacrylate phosphate in PEG hydrogels on mineralization and viability of encapsulated hMSCs. Biomaterials **27,** 1377, 2006.
26. Dadsetan, M., Guda, T., Runge, M.B., *et al.* Effect of calcium phosphate coating and rhBMP-2 on bone regeneration in rabbit calvaria using poly(propylene fumarate) scaffolds. Acta Biomater **18,** 9, 2015.
27. Rosso, F., Giordano, A., Barbarisi, M., and Barbarisi, A. From Cell–ECM interactions to tissue engineering. J Cell Physiol **199,** 174, 2004.
28. Yin Hsu, F., Chueh, S.-C., and Jiin Wang, Y. Microspheres of hydroxyapatite/reconstituted collagen as supports for osteoblast cell growth. Biomaterials **20,** 1931, 1999.
29. Sivakumar, M., and Panduranga Rao, K. Preparation, characterization and in vitro release of gentamicin from coralline hydroxyapatite–gelatin composite microspheres. Biomaterials **23,** 3175, 2002.
30. Cushnie, E.K., Khan, Y.M., and Laurencin, C.T. Amorphous hydroxyapatite-sintered polymeric scaffolds for bone tissue regeneration: physical characterization studies. J Biomed Mater Res Part A **84A,** 54, 2008.

Address correspondence to:
Diederik H.R. Kempen, MD, PhD
Department of Orthopaedic Surgery
Onze Lieve Vrouwe Gasthuis
Oosterpark 9
Amsterdam 1091 AC
The Netherlands

E-mail: d.h.r.kempen@olvg.nl

Received: April 24, 2017
Accepted: October 12, 2017
Online Publication Date: April 20, 2018